A Bacterial Photosynthetic Enzymatic Unit Driving Organic Transistors with Light

Michele Di Lauro, Simona la Gatta, Carlo A. Bortolotti, Valerio Beni, Vitaliy Parkula, Sofia Drakopoulou, Martina Giordani, Marcello Berto, Francesco Milano, Tobias Cramer, Mauro Murgia, Angela Agostiano, Gianluca M. Farinola, Massimo Trotta* and Fabio Biscarini**

Dr. Michele Di Lauro, Prof. Fabio Biscarini
Center for Translational Neurophysiology of Speech and Communication
Istituto Italiano di Tecnologia, 44121 Ferrara (Italy)

Dr. Simona la Gatta, Prof. Gianluca M. Farinola, Prof. Angela Agostiano
Dipartimento di Chimica, Università degli Studi di Bari "Aldo Moro", 70125 Bari (Italy)
E-mail: gianlucamaria.farinola@uniba.it

Dr. Vitaliy Parkula, Sofia Drakopoulou, Dr. Carlo A. Bortolotti, Prof. Fabio Biscarini
Dipartimento di Scienze della Vita, Università di Modena e Reggio Emilia, 41125 Modena (Italy)
E-mail: fabio.biscarini@unimore.it

Dr. Simona la Gatta, Dr. Francesco Milano, Prof. Angela Agostiano, Dr. Massimo Trotta
CNR-IPCF Istituto per i Processi Chimico Fisici, Consiglio Nazionale delle Ricerche, 70125 Bari (Italy)
E-mail: massimo.trotta@cnr.it

Martina Giordani
Dipartimento di Scienze Biomediche, Metaboliche e Neuroscienze, Università di Modena e Reggio Emilia, 41125 Modena (Italy)

Dr. Marcello Berto
Dipartimento di Scienze Biomediche e Chirurgico Specialistiche, Università di Ferrara, 44121 Ferrara (Italy)

Dr. Tobias Cramer
Dipartimento di Fisica e Astronomia, Università degli Studi di Bologna, 40127 Bologna (Italy)

Dr. Mauro Murgia
CNR-ISMN Istituto per lo Studio dei Materiali Nanostrutturati, Consiglio Nazionale delle Ricerche, 40129 Bologna (Italy)

Dr. Valerio Beni
Department of Printed Electronics, RISE Acreo, Research Institute of Sweden, Norrköping 164 40, Sweden

Keywords: Biophotonics, NIR light conversion, photosynthetic reaction center, EGOFET, OECT

Abstract

The photochemical core of every photosynthetic apparatus is the reaction center, a transmembrane enzyme that converts photons into charge-separated states across the biological membrane with an almost unitary quantum yield. We present a light-driven organic transistor architecture, which converts light into electrical current by exploiting the efficiency of this biological machinery. Proper surface tailoring enables the integration of the bacterial reaction center as photoactive element in organic transistors, allowing the transduction of its photogenerated voltage into photomodulation of the output current up to two orders of magnitude. The device architecture, termed Light-driven Electrolyte-Gated Organic Transistor (LEGOT), is the prototype of a new generation of low-power hybrid bio-optoelectronic organic devices.

Main text

Evolution has engineered multi-protein complexes to efficiently convert solar radiation into chemical energy,[1] sustaining the energy needs of life on planet Earth via the photosynthetic process. These photoenzymes catalyze the uphill conversion of oxidized molecules to their reduced forms, using light as energy source. Photosynthetic organisms, such as plants, algae, and some bacteria are the sole kind of organisms on the planet able to harvest and store energy.[2] The photosynthetic anoxygenic bacteria possess a photosynthetic apparatus based on a single functional unit, the reaction center (RC), which converts photons into charge-separated states across the membrane with unmatched quantum yield.

Rhodobacter (*R.*) *sphaeroides* is a purple non-sulphur bacterium, whose RC is a three-subunit transmembrane protein sitting within the photosynthetic membrane.[3] Light impinges a cascade of electron transfer reactions that forms the hole-electron couple with a unitary quantum yield.[4] In absence of exogenous electron donors and acceptors, this state does not evolve further and has a lifetime ranging from hundred milliseconds up to three seconds.[5] See **Figure S1** in the Supporting Information.

This highly efficient photoconverting architecture has spurred numerous mimicking attempts such as photoactive molecules called triads,[6] carefully designed molecular architectures,[7] or the very sophisticated artificial leaf.[8] Recently, bio-hybrid systems encompassing a RC coupled with organic moieties were shown to be efficient transducers of solar radiation.[9–11] RC-based bio-hybrids have been demonstrated in bio-optoelectronics,[12,13] functionally integrated onto devices[14,15] and exploited as active elements in bio-photonic power cells.[16] Here we report the integration of bacterial RC as photoactive element in Electrolyte-Gated Organic Transistors (EGOTs), obtaining photoresponsive bio-hybrid EGOT devices.

EGOTs (**Figure 1**.A), featuring a semiconductive channel exposed to an electrolyte whose potential is fixed by a Gate electrode, are ultra-sensitive sensors towards bio-markers,[17,18] ionic and molecular analytes,[19,20] and transducers of bioelectrical signals.[21,22]

A prototypical bio-organic EGOT, light-gated by means of the photosynthetic RC from *R. sphaeroides*, is presented and termed Light-driven Electrolyte-Gated Organic Transistor - LEGOT.

In the most studied EGOT architectures, namely the Electrolyte-Gated Organic Field-Effect Transistor (EGOFET) and the Organic Electro-Chemical Transistor (OECT), the application of a Gate bias with respect to the grounded Source electrode, V_{GS}, drives ions form the electrolyte towards the organic active materials. This ionic redistribution causes accumulation or depletion of charge carriers in the semiconductive channel, thus modulating the transistor current, I_{DS}, driven by the Drain-Source bias, V_{DS}. The gating capacitance in EGOTs is large,[23,24] hence small variations of the charge distribution at the Gate/electrolyte interface result into large I_{DS} variations, therefore EGOT sensors usually rely on Gate functionalization.[25–27]

LEGOT, accordingly, exploits photogenerated charge redistribution to modulate I_{DS}.

In LEGOT, RC is adsorbed on an Indium Tin Oxide (ITO) Gate electrode and the channel is either a solution processed 6,13-Bis(triisopropylsilylethynyl) pentacene (TIPS-P5) layer or a

printed poly(3,4-ethylenedioxythiophene):poly(styrenesulfonate) (PEDOT:PSS) film, for EGOFET and OECT architectures, respectively. The device is depicted in Figure 1.B-D.

The RC photoconversion ability is driven by the efficient absorption of photons in the range 250 – 950 nm,[28,29] in particular in the near-IR range (NIR). Since both active materials are NIR transparent,[30,31] NIR-excitation allows to unambiguously ascribe photoinduced effects to the sole RC.

The major issue in the deposition of RC on ITO Gate is the random orientation of light-generated dipoles,[32,33] which would result in null net potential variation. Control of RC orientation, a compulsory requirement to provide an additional gating effect, can be obtained by casting a layer of oxidized horse hearth cytochrome *c* (cyt) on the ITO surface. Cyt is a redox protein that, in its reduced form, acts as physiological electron donor to the photogenerated hole within the RC. This transfer requires binding of the cyt to the specific docking site on the RC periplasmic face,[34] arising from purely electrostatic interactions and independent on the redox state of the cyt.[35] In its oxidized form, cyt can be used to preferentially orient the RC on the surface of the ITO Gate, albeit avoiding faradaic currents associated with electron transfer reactions.

This approach has been exploited in LEGOT light-sensitive unit, by casting a layer of oxidized cyt onto the ITO Gate, prior to RC deposition, to induce an orientation of the photoenzyme, as shown in Figure 1.E.

The process was monitored via Atomic Force Microscopy, Figure 1.G-I, showing the formation of a compact layer of cyt (Figure 1.H) and the presence of RC aggregates onto the cyt matrix after two consecutive deposition steps (Figure 1.I).

Light-sensitive unit was characterized by surface photovoltage spectroscopy, monitoring the surface potential at different wavelengths. The normalized photovoltage spectrum, shown in **Figure 2**, exhibits close similarity to the absorption spectrum of the RC. Surface potential has been further investigated by means of chronopotentiometry, in light-dark cycles (λ = 802 nm),

as shown in **Figure 3**.A. Upon illumination, the light sensitive unit potential negatively shifts ($\Delta V = 55 \pm 9$ mV) on a relatively slow timescale ($\tau = 18 \pm 5$ s), longer than the normal lifetime of the hole-electron couple (between 100 ms and 3 s). This is due to the accumulation, induced by continuous illumination, of usually negligible transient species in the RC having much longer lifetime. The relative weight of these slower phenomena is artificially increased when the experimental setups have a lower collection rate than the fast component of the recombination time.[36]

For LEGOT characterization, transfer characteristics have been acquired continuously. During acquisition, the light excitation source has been switched ON and OFF every 200 s. The time evolution of transfer characteristics is reported in Figure 3.B and Figure 3.C for TIPS-P5 and PEDOT:PSS devices, respectively.

In both cases, the light-induced negative Gate potential shift results in higher current upon illumination, although the rationale is different. In accumulation EGOFET, a more negative Gate potential causes larger (negative) currents, inducing more holes in the semiconductive channel. In depletion OECT, the current increase is ascribed to the decreased positive Gate voltage, which injects a smaller amount of cations in the semiconductive channel. In EGOFETs the negative chronopotentiometric shift results in a positive shift of the threshold voltage, V_{th}, ($\Delta V_{th} = 52 \pm 3$ mV, Figure 3.D). It is possible to exploit this phenomenon to drive the device by the sole use of light. In the dark, a V_{GS} of -0.5 V, less negative than V_{th}, does not turn the device ON. Upon illumination, V_{th} is crossed and the device responds with a 20-fold current increase, Figure 3.E. The analogous experiment in OECTs, Figure 3.F, shows a current increase as high as 25 µA upon illumination.

At 802 nm only RC exhibits significant absorption,[3,29–31,37,38] hence the observed phenomena are due to the additional gating effect of photogenerated oriented dipoles at the Gate/Electrolyte interface. This additional unscreened negative charge distribution at the Gate shifts its

electrochemical potential and modulates the charge carrier density in the semiconductive channel.

In conclusion, building on the EGOT's nature of interfacial charge/voltage amplifiers, RC functionalized EGOTs technologically exploit the transduction capability of the photoenzyme in the NIR, leading to a novel bio-based low-power device, here termed LEGOT, that enables light-driven amplification of current in aqueous environment.

Experimental Section

TIPS-P5 EGOT fabrication: Au Source and Drain interdigitated electrodes were deposited onto quartz substrates by photolithography and lift-off (FBK, Trento, Italy), obtaining a 15 µm long and 7.5 mm wide channel. TIPS-P5 was deposited onto these piraña-etched substrates via spin coating of a 1% w/w solution in a 8:2 mixture of Toluene and n-Hexane and thermally cured.

PEDOT:PSS EGOT fabrication: Devices were manufactured by screen-printing on PET foils (Polyfoil Bias), thermally treated prior to use (140 °C, 45 min). Silver tracks and carbon contact pads have been printed using Ag5000 silver ink (DuPont, UK) and a commercial carbon ink (C2130307D1, Gwent, UK), respectively. Clevios^{TM} SV3 PEDOT:PSS ink (Heraeus Group, Germany) was used to print the transistor channel.

Reaction center production/extraction: The RC was isolated and purified from cultured *Rhodobacter sphaeroides* and its integrity and activity were checked by UV-Vis-NIR spectroscopy and by flash induced absorbance change measurements performed on an instrument of local design.[9,39,40]

Light-sensitive Gate fabrication: 4 nmol of horse hearth cytochrome *c* (Sigma-Aldrich, CAS: 9007-43-6) in phosphate 20 mM, Triton X-100 0.03%, EDTA 1 mM buffer (pH=8) were drop-cast onto ITO. After drying, 0.73 nmol of RC in the same buffer were casted, to a final ratio of 5.5 cyt:RC.

Photovoltage Spectroscopy: Photovoltage spectra were acquired in a home-built setup (See **Figure S2** in the Supporting Information).

Chronopotentiometry: V vs t curves were acquired using a CHI760C potentiostat in a two electrode configuration, using the light-sensitive unit as working electrode.

LEGOT characterization: Electrical measurements were performed using a Source-Measure Unit (Agilent-B2912A) and a custom designed software, in common ground configuration, in a 20 mM phosphate-buffer (pH = 8). NIR excitation has been provided using an Osram LED (802 nm, 2.1 W).

Control Experiments: See **Figure S3** in the Supporting Information.

Supporting Information
Supporting Information is available from the Wiley Online Library or from the author.

Acknowledgements
Michele Di Lauro and Simona la Gatta contributed equally to this work. The authors would like to acknowledge Ms. Marie Nilsson and Mr. Lorenz Theuer for design and fabrication of the PEDOT:PSS channel. The authors would also aknowledge EuroNanoMed-III AMI project, Life Science Department of UNIMORE through "FAR 2015", Marie Curie ETN project iSwitch (GA No. 642196), Swedish Foundation for Strategic Research (Smart Intra-body network; grant RIT15-0119) and EU project 800926 (HyPhOE) for funding.

Received: ((will be filled in by the editorial staff))
Revised: ((will be filled in by the editorial staff))
Published online: ((will be filled in by the editorial staff))

References

[1] W. F. Martin, D. A. Bryant, J. T. Beatty, *FEMS Microbiol. Rev.* **2018**, *42*, 205.

[2] J. P. Allen, J. C. Williams, *FEBS Lett.* **1998**, 5.

[3] G. Feher, J. P. Allen, M. Y. Okamura, D. C. Rees, *Nature* **1989**, *339*, 111.

[4] C. A. Wraight, R. K. Clayton, *BBA - Bioenerg.* **1974**, *333*, 246.

[5] L. Nagy, F. Milano, M. Dorogi, A. Agostiano, G. Laczkó, K. Szebényi, G. Váró, M.

Trotta, P. Maróti, *Biochemistry* **2004**, *43*, 12913.

[6] M. R. Wasielewski, G. L. Gaines, G. P. Wiederrecht, W. A. Svec, M. P. Niemczyk, *J. Am. Chem. Soc.* **1993**, *115*, 10442.

[7] F. Puntoriero, A. Sartorel, M. Orlandi, G. La Ganga, S. Serroni, M. Bonchio, F. Scandola, S. Campagna, *Coord. Chem. Rev.* **2011**, *255*, 2594.

[8] D. G. Nocera, *Acc. Chem. Res.* **2012**, *45*, 767.

[9] F. Milano, R. R. Tangorra, O. Hassan Omar, R. Ragni, A. Operamolla, A. Agostiano, G. M. Farinola, M. Trotta, *Angew. Chemie - Int. Ed.* **2012**, *51*, 11019.

[10] J. Liu, J. Mantell, N. Di Bartolo, M. R. Jones, *Small* **2018**, *1804267*, 1804267.

[11] V. M. Friebe, J. D. Delgado, D. J. K. Swainsbury, J. M. Gruber, A. Chanaewa, R. Van Grondelle, E. Von Hauff, D. Millo, M. R. Jones, R. N. Frese, *Adv. Funct. Mater.* **2016**, *26*, 285.

[12] A. Operamolla, R. Ragni, F. Milano, R. Roberto Tangorra, A. Antonucci, A. Agostiano, M. Trotta, G. Farinola, *J. Mater. Chem. C* **2015**, *3*, 6471.

[13] F. Milano, A. Punzi, R. Ragni, M. Trotta, G. M. Farinola, *Adv. Funct. Mater.* **2018**, *1805521*, 1805521.

[14] E. D. Głowacki, R. R. Tangorra, H. Coskun, D. Farka, A. Operamolla, Y. Kanbur, F. Milano, L. Giotta, G. M. Farinola, N. S. Sariciftci, *J. Mater. Chem. C* **2015**, *3*, 6554.

[15] N. Terasaki, N. Yamamoto, K. Tamada, M. Hattori, T. Hiraga, A. Tohri, I. Sato, M. Iwai, M. Iwai, S. Taguchi, I. Enami, Y. Inoue, Y. Yamanoi, T. Yonezawa, K. Mizuno, M. Murata, H. Nishihara, S. Yoneyama, M. Minakata, T. Ohmori, M. Sakai, M. Fujii, *Biochim. Biophys. Acta - Bioenerg.* **2007**, *1767*, 653.

[16] S. K. Ravi, P. Rawding, A. M. Elshahawy, K. Huang, W. Sun, F. Zhao, J. Wang, M. R. Jones, S. C. Tan, *Nat. Commun.* **n.d.**, 1.

[17] J. Rivnay, P. Leleux, M. Ferro, M. Sessolo, A. Williamson, D. a. Koutsouras, D. Khodagholy, M. Ramuz, X. Strakosas, R. M. Owens, C. Benar, J.-M. Badier, C.

Bernard, G. G. Malliaras, *Sci. Adv.* **2015**, *1*, e1400251.

[18] M. Berto, C. Diacci, R. D'Agata, M. Pinti, E. Bianchini, M. Di Lauro, S. Casalini, A. Cossarizza, M. Berggren, D. Simon, G. Spoto, F. Biscarini, C. A. Bortolotti, *Adv. Biosyst.* **2017**, *1700072*, 1700072.

[19] M. Y. Mulla, E. Tuccori, M. Magliulo, G. Lattanzi, G. Palazzo, K. Persaud, L. Torsi, *Nat. Commun.* **2015**, *6*, 6010.

[20] M. Berto, C. Diacci, L. Theuer, M. Di Lauro, D. T. Simon, M. Berggren, F. Biscarini, V. Beni, C. A. Bortolotti, *Flex. Print. Electron.* **2018**, *3*, DOI 10.1088/2058-8585/aac8a8.

[21] A. Campana, T. Cramer, D. T. Simon, M. Berggren, F. Biscarini, *Adv. Mater.* **2014**, *26*, 3874.

[22] D. Khodagholy, J. N. Gelinas, T. Thesen, W. Doyle, O. Devinsky, G. G. Malliaras, G. Buzsáki, *Nat. Neurosci.* **2015**, *18*, 310.

[23] A. Volkov, K. Wijeratne, E. Mitraka, U. Ail, D. Zhao, J. W. Andreasen, M. Berggren, X. Crispin, **2017**, *27*.

[24] G. Palazzo, D. De Tullio, M. Magliulo, A. Mallardi, F. Intranuovo, M. Y. Mulla, P. Favia, I. Vikholm-Lundin, L. Torsi, *Adv. Mater.* **2015**, *27*, 911.

[25] M. Berto, S. Casalini, M. Di Lauro, S. L. Marasso, M. Cocuzza, D. Perrone, M. Pinti, A. Cossarizza, C. F. Pirri, D. T. Simon, M. Berggren, F. Zerbetto, C. A. Bortolotti, F. Biscarini, *Anal. Chem.* **2016**, *88*, 12330.

[26] M. Magliulo, A. Mallardi, R. Gristina, F. Ridi, L. Sabbatini, N. Cioffi, G. Palazzo, L. Torsi, *Anal. Chem.* **2013**, *85*, 3849.

[27] F. Cicoira, M. Sessolo, O. Yaghmazadeh, J. a DeFranco, S. Y. Yang, G. G. Malliaras, *Adv. Mater.* **2010**, *22*, 1012.

[28] E. Altamura, F. Milano, R. R. Tangorra, M. Trotta, O. H. Omar, P. Stano, F. Mavelli, *Proc. Natl. Acad. Sci.* **2017**, *114*, 3837.

[29] G. Feher, *Photochem. Photobiol.* **1971**, *14*, 373.

[30] S. Kazim, F. J. Ramos, P. Gao, M. K. Nazeeruddin, M. Grätzel, S. Ahmad, *Energy Environ. Sci.* **2015**, *8*, 1816.

[31] Z. Cao, Z. Chen, L. Escoubas, *Opt. Mater. Express* **2014**, *4*, 2525.

[32] V. K. Singh, S. K. Ravi, J. W. Ho, J. K. C. Wong, M. R. Jones, S. C. Tan, *Adv. Funct. Mater.* **2018**, *28*, 1.

[33] E. D. Głowacki, G. Romanazzi, C. Yumusak, H. Coskun, U. Monkowius, G. Voss, M. Burian, R. T. Lechner, N. Demitri, G. J. Redhammer, N. Sünger, G. P. Suranna, S. Sariciftci, *Adv. Funct. Mater.* **2015**, *25*, 776.

[34] H. L. Axelrod, E. C. Abresch, M. Y. Okamura, A. P. Yeh, D. C. Rees, G. Feher, *J. Mol. Biol.* **2002**, *319*, 501.

[35] L. Gerencsér, G. Laczkó, P. Maróti, *Biochemistry* **1999**, *38*, 16866.

[36] A. Agostiano, F. Milano, M. Trotta, *Photosynth. Res.* **2005**, *83*, 53.

[37] M. H. Stowell, T. M. McPhillips, D. C. Rees, S. M. Soltis, E. Abresch, G. Feher, *Science (80-.).* **1997**, *276*, 812.

[38] J. Luo, D. Billep, T. Waechtler, T. Otto, M. Toader, O. Gordan, E. Sheremet, J. Martin, M. Hietschold, D. R. T. Zahn, T. Gessner, *J. Mater. Chem. A* **2013**, *1*, 7576.

[39] F. Milano, F. Italiano, A. Agostiano, M. Trotta, *Photosynth Res* **2009**, 107.

[40] F. Milano, A. Agostiano, F. Mavelli, M. Trotta, *Eur. J. Biochem.* **2003**, *270*, 4595.

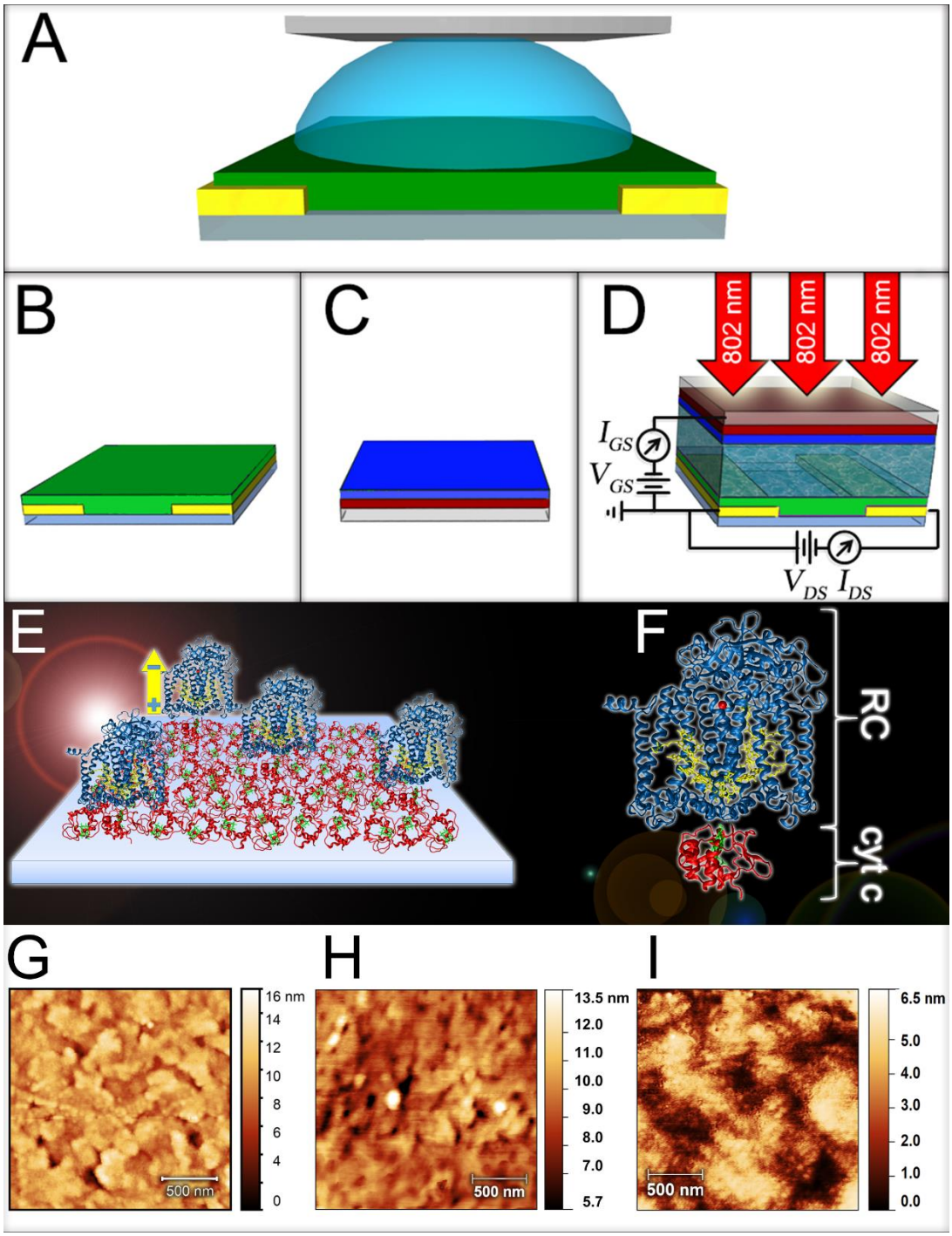

Figure 1. A) Conceptual scheme of a generic top-gate bottom-contact EGOT device, showing gold source and drain electrodes (yellow) patterned on a substrate (grey) and bridged by a semiconductor thin-film (green). The channel is exposed to an electrolyte solution, whose potential is fixed by a metallic plate (light grey); B-D) Schematic representation of the functional units of LEGOT: transduction element, featuring the channel of an EGOT with source and drain contacts (B); light sensitive element, made of a transparent ITO Gate electrode (grey) coated with cyt (red) and RC (blue) (C); final LEGOT layout with transducing and light sensitive elements coupled by the electrolyte solution, with sketched illumination path and electrical connections (D); E) oxidized form of cyt is deposited by drop-casting on the ITO surface; RC is successively deposited by drop-casting on top of the cyt layer; the orientation of the photoinduced dipole is highlighted (yellow arrow); B) crystallographic structure obtained for the complex cytochrome c-RC;[34] C-D-E) 2 μm x 2 μm Atomic Force Microscopy topographies of bare ITO (C), ITO with cyt (D) and ITO with cyt and RC (E).

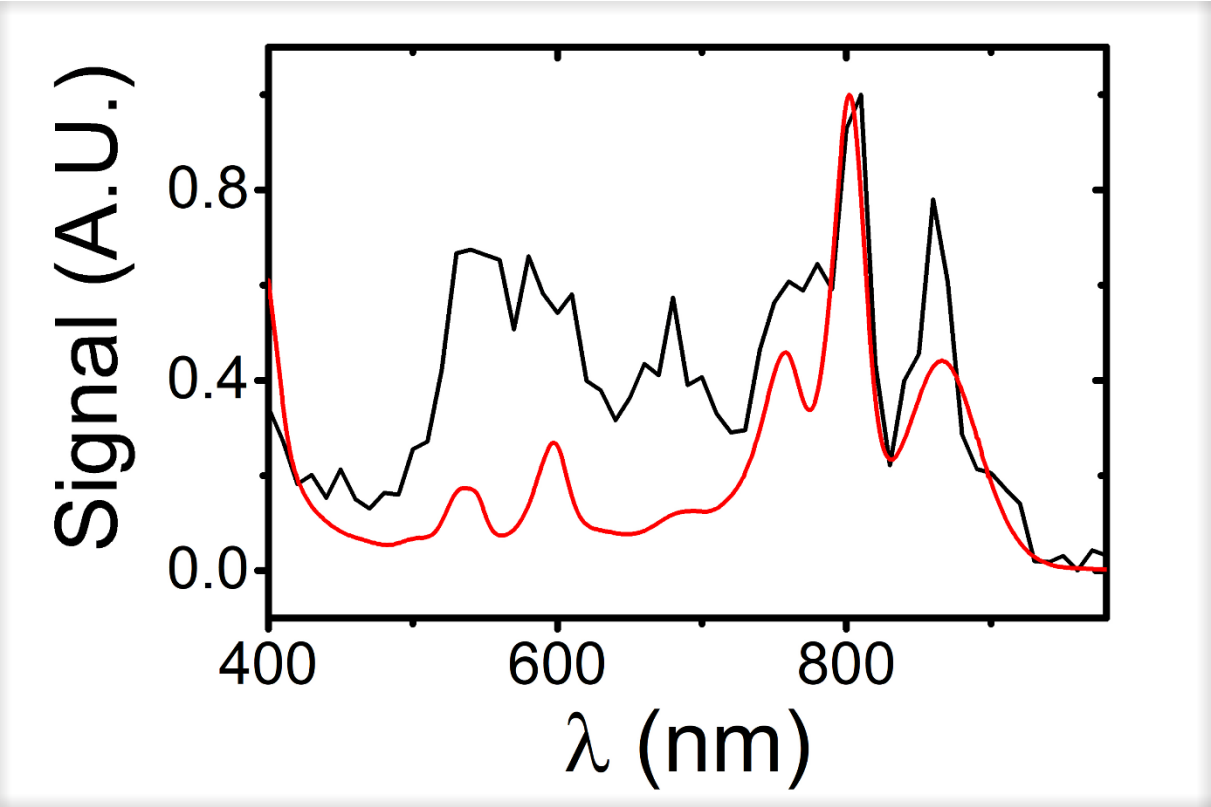

Figure 2. Absorption spectrum of RC in solution (red) and normalized photovoltage spectrum of the light-sensitive unit of the EGOT (black).

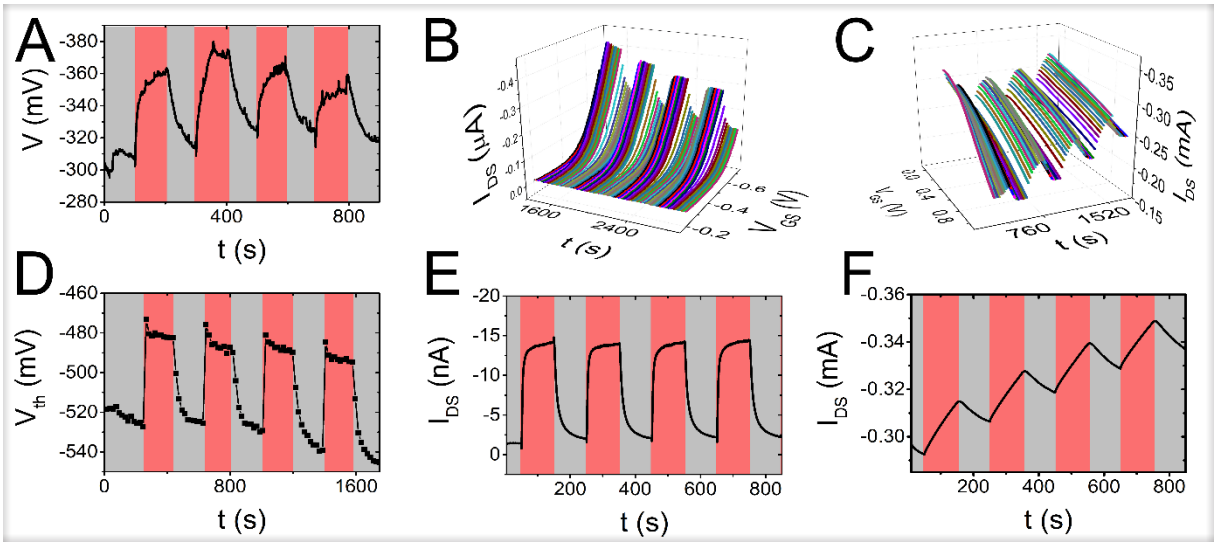

Figure 3. A) Chronopotentiometry of the light-sensitive element. Illumination with a NIR (λ=802 nm) LED negatively shifts the electrode potential; B-C) I_{DS} vs V_{GS} vs time plots showing evolution of transfer characteristics of TIPS-P5 (B) and PEDOT:PSS (C) devicese upon dark-light cycles; D) Threshold voltage of TIPS-P5 EGOT; E) I_{DS} vs t plot of TIPS-P5 EGOT (V_{DS} = -0.5 V, V_{GS} = -0.5 V); F) I_{DS} vs t plot of PEDOT:PSS EGOT (V_{DS} = -0.5 V, V_{GS} = 0.3 V)

The Light-driven Electrolyte-Gated Organic Transistor – LEGOT – is herein demonstrated. This architecture, obtained by integration of the photosynthetic reaction center of *Rhodobacter sphaeroides* onto a transparent Gate electrode, yields current amplification under NIR photoexcitation. Photoinduced biomodulation of the interfacial potential contributes to the device gating, yielding a low-power technological tool for direct conversion of solar light into current.

Keyword Organic Bio-Photonics

Michele Di Lauro, Simona la Gatta, Carlo A. Bortolotti, Valerio Beni, Vitaliy Parkula, Sofia Drakopoulou, Martina Giordani, Marcello Berto, Francesco Milano, Tobias Cramer, Mauro Murgia, Angela Agostiano, Gianluca M. Farinola*, Massimo Trotta* and Fabio Biscarini*

A Bacterial Photosynthetic Enzymatic Unit Driving Organic Transistors with Light

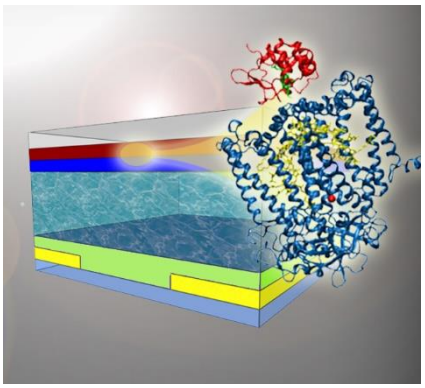

Supporting Information

A Bacterial Photosynthetic Enzymatic Unit Driving Organic Transistors with Light

Michele Di Lauro, Simona la Gatta, Carlo A. Bortolotti, Valerio Beni, Vitaliy Parkula, Sofia Drakopoulou, Martina Giordani, Marcello Berto, Francesco Milano, Tobias Cramer, Mauro Murgia, Angela Agostiano, Gianluca M. Farinola, Massimo Trotta* and Fabio Biscarini**

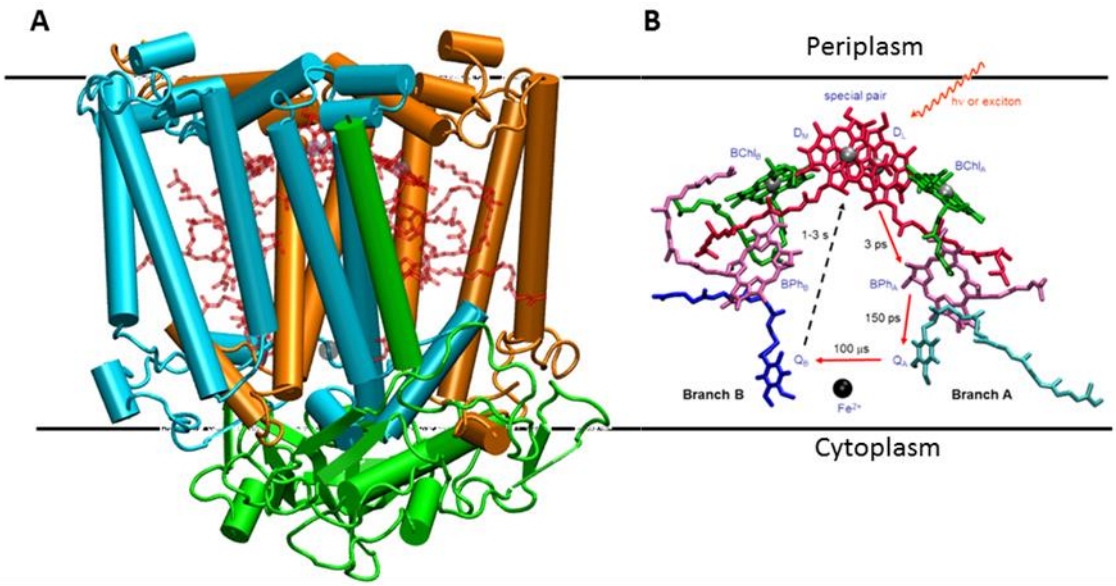

Figure S1. Three-dimensional structure of the photosynthetic reaction center (A) from *Rhodobacter sphaeroides* obtained by crystallographic data (Pdb code A1IJ). The protein is formed by three subunits. One hydrophilic subunit (H, in green), anchored to the rest of the enzyme by one alfa-helix, and two hydrophobic subunits (L and M in cyan and orange respectively). Subunits L and M span the entire membrane thickness, from the periplasm to the cytoplasm, for roughly four nm. B) Spatial organization of the nine cofactors responsible for the intra-protein electron transfer. The cofactors are organized along two branches, *A* and *B*. The electron generated by the absorption of a photon travels along the sole *A* branch from the special pair (or dimer, in red) sitting close to the periplasm and formed by two excitonically coupled bacteriochlorophylls. The electron moves from the dimer D to reach the monomeric bacteriochlorophyll (in green), leaving a positive charge sitting on the dimer. The electron further reaches a monomeric bacteriopheophytin (in purple), then a tightly bond quinone named Q_A (in cyan) that functions as first electron acceptor. A second loosely bound quinone belonging to the *B* branch, and hence named Q_B (in blue), functions as final electron acceptor. In absence of exogenous electron donors and acceptors, the fate of the hole-electron couple $D^+Q_B^-$ is to recombine to the ground state of the protein within 1 second. In case the final electron acceptor Q_B is either removed or inhibited, the time required for the recombination from the $D^+Q_A^-$ state drops to 100 ms.

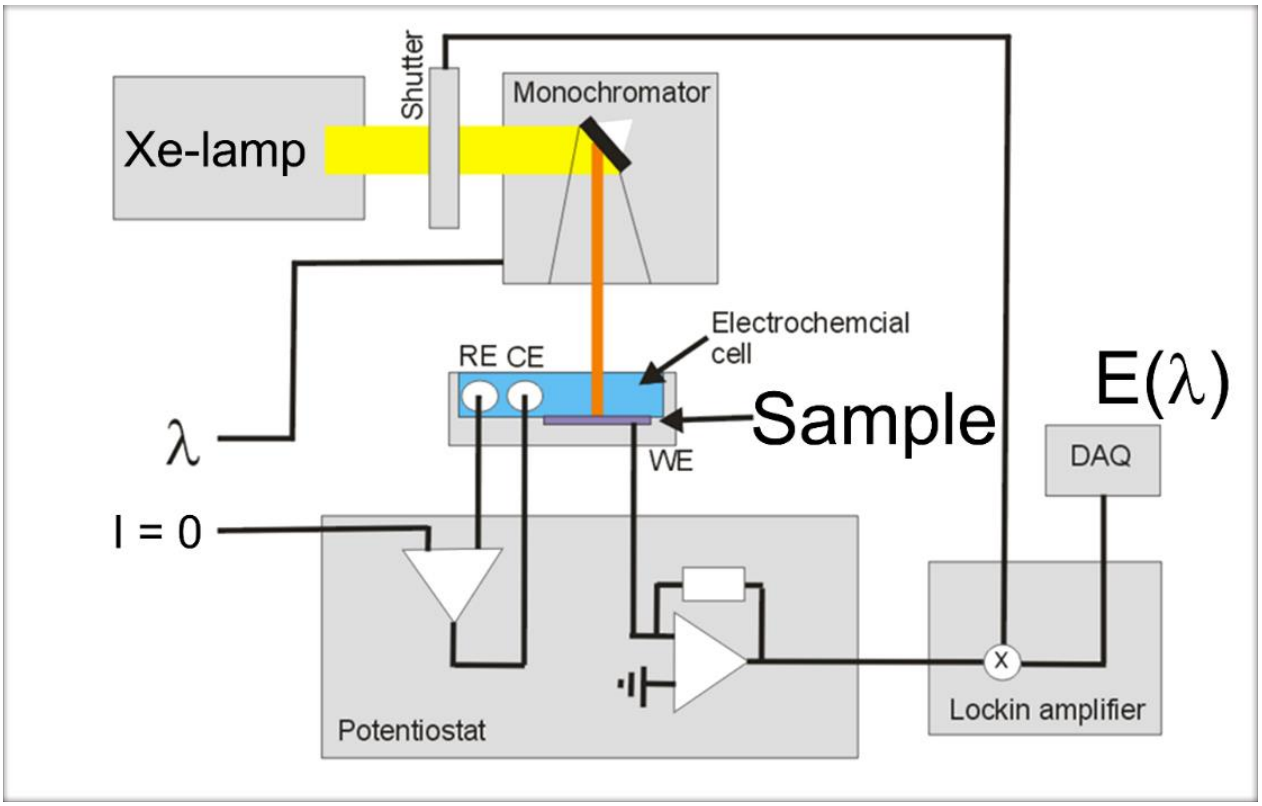

Figure S2. **Photovoltage spectroscopy setup**. A standard electrochemical cell with quartz windows, comprising a refererence Ag/AgCl electrode (RE) and a platinum counter electrode (CE), operated in current control (I = 0) under illumination, allows to measure the voltage variations (E) at our modified gate electrode (WE) as a function of the excitation wavelength (λ). The signal, E(λ), from the potentiostat is then amplified and transferred to a digital acquisition (DAQ) unit

Control Experiments

To unambiguously ascribe the observed amplification effect to the bio-functionalization of the Gate electrode, a set of control experiments using TIPS-P5 EGOTs has been performed. Choosing the maximum I_{DS} of the first acquired transfer characteristic for each device, $I_{DS,MAX}(0)$, as a reference state, it is possible to define the relative signal variation, S, as follows:

$$S = \frac{I_{DS,MAX}(t) - I_{DS,MAX}(0)}{I_{DS,MAX}(0)};$$

this definition of signal allows a direct comparison between light responses of different devices. In Figure S1 we superimpose the time evolution of the signal variation of the proposed LEGOT (black squares) and a control EGOT, the latter with bare ITO gate electrode (blue triangles). It is clear that the control EGOT with bare ITO is light-insensitive, emphasizing that the oriented RC layer is responsible of the LEGOT light sensitivity. In a further control experiment, an EGOT built by casting RC onto ITO without the cyt *c* orienting layer shows no current modulation under illumination (red dots). A last control is the device with the sole cyt *c* gate functionalization (green triangles) that also does not exhibit any modulation induced by light.

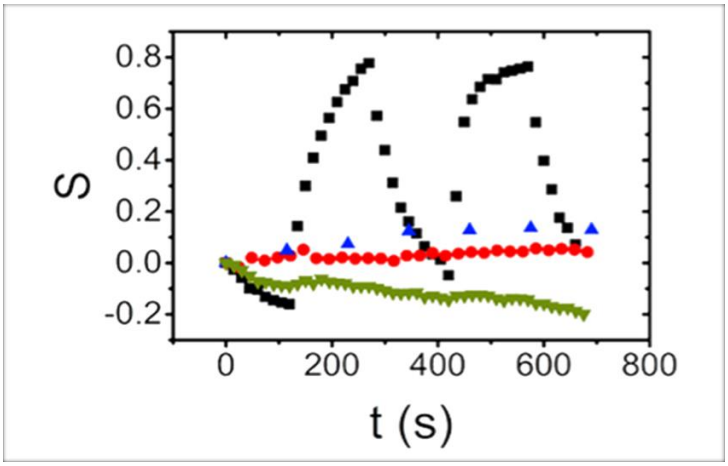

Figure S3. Control experiments. Relative signal variations, *S*, of the proposed LEGOT (black squares), LEGOT with randomly oriented RC on the Gate (red dots), control EGOTs featuring a bare ITO Gate (blue triangles) and a cyt *c*-functionalized ITO Gate (green triangles).